Excited State Properties of C_6H_6 and C_6D_6 Studied by Feynman Path Integral−ab Initio Simulations

Michael C. Böhm*

Institut für Physikalische Chemie, Physikalische Chemie III, Technische Universität Darmstadt, Petersenstr. 20, D-64287 Darmstadt, Germany

Joachim Schulte

Bruker Analytik GmbH, Silberstreifen, D-76287 Rheinstetten, Germany

Rafael Ramírez*

Instituto de Ciencia de Materiales, Consejo Superior de Investigaciones Cientificas, Campus Cantoblanco, E−28049 Madrid, Spain

Received: September 12, 2001; In Final Form: January 3, 2002

The Feynman path integral Monte Carlo formalism has been combined with an ab initio configuration interaction approach in order to analyze the excited singlet states of the benzene isomers C_6H_6 and C_6D_6 under the conditions of thermal equilibrium. Electronic transition energies $^{PI}\bar{E}_T$ and oscillator strength $^{PI}\bar{f}_{osc}$, which have been sampled over large sets of nuclear configurations, are compared with single-configuration results E_T, f_{osc}. The latter set of quantities has been derived for the D_{6h} energy minimum of benzene. The present quantum Monte Carlo simulations lead to a simple physical picture for the nonzero intensities of the transitions to the two lowest excited singlet states of the two benzene isomers. Under D_{6h} conditions, the transitions to the $^1B_{2u}$ and $^1B_{1u}$ states are dipole-forbidden. The influence of the nuclear degrees of freedom on the excited-state properties of the two π rings up to room temperature is quantum driven. The quantum fluctuations of the nuclei on a potential energy surface with large anharmonicities lead to a sizable redistribution of the transition intensities. At the same time they lower the transition energies $^{PI}\bar{E}_T$ relative to the E_T numbers at the energy minimum. Transitions, which are dipole-allowed for the rigid D_{6h} symmetry of C_6H_6 and C_6D_6, lose intensity under the influence of the nuclear fluctuations; vice versa for transitions dipole-forbidden under the constraints of the point group D_{6h}. The temperature and isotope dependence of these effects is discussed. Inherent problems of excited-state calculations of molecules on the basis of a single nuclear configuration are emphasized.

I. Introduction

Quantum chemical methods have become an important and rather powerful computational tool for the analysis of the electronic structure of atoms, molecules and solids. Accurate determinations of ground-state properties of molecules with the help of ab initio methods are accessible for a number of years.[1−3] High-quality calculations of molecular electronic excited states on the basis of ab initio techniques are less established. The growing computational facilities of the past years, however, have provided the technical prerequisites for the development of elaborate ab initio approaches to study molecular electronic excited states. The theoretical methods employed are either of the post Hartree−Fock (HF) or density functional (DF) type.

The vibrational broadening of molecular electronic transitions, however, indicates that the pure consideration of the electronic degrees of freedom is insufficient to understand the excited-state properties of molecules quantitatively. The interplay between the electronic and nuclear degrees of freedom has been studied both by experimentalists and theoreticians. The first contributions on the vibrational broadening of electronic transitions go back to Herzberg[4] who had employed group theoretical methods to explain the coupling between nuclear modes and electronic transitions. The work of Herzberg has led to widely adopted phenomenological concepts such as "vibrational borrowing" of transition intensities; see below. A number of sophisticated techniques to consider the nuclear degrees of freedom in molecular electronic transitions has been reported in the past two decades. Heller et al.[5−7] have developed Gaussian wave packet approaches to simulate the temperature (T) and isotope dependence of electronic absorption spectra. Schinke et al.[8−10] have described multidimensional reflection principles to take into account the influence of the nuclear degrees of freedom on electronic transitions. Most of the simulations presented in refs 8−10 are of a semiclassical type. Other theoretical methods to consider the vibronic coupling in electronic absorptions can be found in refs 11−18. The consideration of anharmonicities on the potential energy surface (PES), however, remains an exception in the above studies. An ab initio quantum molecular dynamics approach beyond the simple harmonic approximation has been developed by Ben-Nun and Martínez.[17]

Despite the impressive progress in the development of vibronic coupling theories, we still have the situation that the majority of excited *and* ground state calculations of molecules is performed for space-fixed nuclear coordinates. Vibrational corrections in connection with ab initio calculations are sparse exceptions. Electronic structure approaches on the basis of only *one* space-fixed set of nuclear coordinates define the so-called crude Born−Oppenheimer (CBO) approximation[19] which is based on a complete decoupling of the electronic and nuclear degrees of freedom. The configuration at the minimum of the

10.1021/jp013483h CCC: $22.00
Published on Web 03/07/2002

potential energy surface is a widely adopted standard in the CBO hierarchy. The atomic positions of this structure are mapped by the 3n-dimensional vector $\mathbf{R_o}$ with *n* symbolizing the number of atoms. The electronic wave function $\Psi_{el}(\mathbf{r}_{el})$ in the CBO approximation depends only parametrically on the nuclear coordinates $\mathbf{R_o}$. In the present work, this behavior has been expressed by the symbol $\Psi_{el}(\mathbf{r}_{el},\mathbf{R_o})$. The vector $\mathbf{r}_{el}$ defines the electronic coordinates. The symbol $\mathbf{R}$ has been used to map the nuclear coordinates for configurations which differ from the PES minimum. The $\mathbf{R_o}$ geometry is not only adopted in ground state calculations. It is also widely employed in theoretical studies of molecular electronic excited states, a choice which has its origin in the highest intensities of the so-called vertical Franck−Condon (FC) transitions.[20,21] To sum up; the atomic nuclei in the CBO approximation are treated as space-fixed particles. Neither their classical (thermal) nor their quantum degrees of freedom are taken into account in quantum chemical calculations of the single nuclear configuration type.

In the present work, we have studied the excited-state properties of the benzene isomers C_6H_6 and C_6D_6 under the conditions of thermal equilibrium, i.e., under explicit consideration of the nuclear degrees of freedom. Benzene is a popular model system in chemistry for understanding excited states.[22] The number of papers on C_6H_6 is legion, where the capabilities and failures of post HF and DF approaches as well as basis set problems for the analysis of excited states have been discussed in detail.[23−31] Note that the theoretical works in refs 23−31 are all based on the CBO approximation which implies that the electronic excitation energies and their intensities have been evaluated for the vibrationless $\mathbf{R_o}$ geometry of benzene in the electronic ground state. The oscillator strength f_{osc} of a given electronic transition in this approximation is determined by the molecular point symmetry at the minimum of the PES. In the case of C_6H_6 and C_6D_6 it is the point symmetry D_{6h}.

As a result of symmetry-forbidden valence states, the optical spectrum of benzene is a challenge both for experimentalists and theorists.[22] This hydrocarbon molecule has been the first example where such forbidden states have been observed by a number of spectroscopists. The early measurements have been reviewed by Herzberg.[4] For further experimental information see refs 32−35. The $\pi \rightarrow \pi^*$ transitions to the two lowest singlet states of benzene of $^1B_{2u}$ and $^1B_{1u}$ symmetry are dipole-forbidden under D_{6h} conditions. Both excited singlet states arise from transitions from the doubly degenerated highest occupied molecular orbital (HOMO) to the doubly degenerated lowest unoccupied MO (LUMO). The two MO wave functions belong to the irreducible representations e_{1g} and e_{2u}. The nonzero intensity of these singlet transitions has been explained by vibronic coupling theories as well as by vibronic borrowing.[4] Ab initio calculations on the vibronic coupling in benzene are still missing. As a result of the sizable temperature dependence of the intensities of the $^1B_{2u}$ and $^1B_{1u}$ transitions, these bands have been denoted as "hot bands".[4]

For the present theoretical investigation of the excited-state properties of C_6H_6 and C_6D_6 in thermal equilibrium, we have employed the Feynman path integral quantum Monte Carlo (PIMC) technique.[36−40] This approach from statistical mechanics has been combined with an electronic ab initio Hamiltonian. The excited-state properties of the two benzene isomers have been investigated via an ensemble averaging over large sets of nuclear (ground state) configurations which are populated in thermal equilibrium. In contrast to the majority of the above-mentioned theories to consider the nuclear degrees of freedom in molecular electronic transitions, the present PIMC approach goes beyond the simple harmonic approximation. In recent contributions, we have adopted PIMC−ab initio implementations to derive ground-state properties of molecules under explicit consideration of the nuclear degrees of freedom.[41−47] These quantum Monte Carlo (QMC) studies as well as the stimulating PI molecular dynamics investigations of other authors[48−52] have shown that the influence of the nuclear fluctuations on the expectation values of the electronic Hamiltonian is particularly large in molecules with light atoms. This, however, implies that the anharmonicities on the PES become of sizable influence.

The generation of large sets of nuclear configurations described by vectors $\mathbf{R}$ is a key-step in the PIMC−ab initio simulations described in refs 41−47. The population of these configurations follows a canonical ensemble statistics. In the present work, we make use of the symbol $X(\mathbf{R})$ to denote that a given (electronic) quantity *X* has been determined for a nuclear configuration described by the vector $\mathbf{R}$. The overall ensemble $X(\mathbf{R})$ maps the vibrationally broadened distribution function of *X*. Integration (or summation) of the $X(\mathbf{R})$ over the members of the QMC ensemble yields the statistical mean value $\bar{X}$ ($^{PI}\bar{X}$) of quantity *X*. The symbols *X* and $\bar{X}$ ($^{PI}\bar{X}$) will be used throughout in the present work to discriminate the expectation values of the single-configuration type X ($\equiv X(\mathbf{R})$) from the QMC based ensemble averages $\bar{X}$ ($^{PI}\bar{X}$). The difference between the quantities $\bar{X}$ and $^{PI}\bar{X}$ will be explained in the following theory section.

It is the time-scale of a spectroscopic measurement which determines whether we observe the distribution function $X(\mathbf{R})$ of a given quantity *X* or the thermal mean value. Both sets of quantities can be derived by PIMC calculations. In the present work, we have used PIMC−ab initio simulations to evaluate vibrationally broadened distribution functions of electronic transitions together with the FC maxima in thermal equilibrium. This capability of the PIMC formalism makes it possible to compare the excited-state properties of C_6H_6 and C_6D_6 in the single nuclear configuration picture of the CBO approximation with quantities derived in thermal equilibrium. On the basis of the above discussion, it is clear that any difference between the two sets of theoretical numbers is a manifestation of a vital physical effect included in the total molecular Hamiltonian, i.e., the vibronic coupling between electrons and nuclei. This interaction is neglected in studies of the CBO type no matter how large the effort in the design of the H_{el} has been. The present PIMC−ab initio formalism can be considered as an adiabatic Born−Oppenheimer (ABO) approach,[19] a theoretical tool which goes beyond the single-configuration picture of the CBO approximation. Consideration of all vibronic coupling elements in the above cited perturbational expansions[11−14] would lead to a one-to-one correspondence between the present nonperturbational technique and previous vibronic coupling theories.

The excitation energies E_T, $^{PI}\bar{E}_T$ and oscillator strengths f_{osc}, $^{PI}\bar{f}_{osc}$ in the present QMC work have been determined by a configuration interaction (CI) scheme covering singly (S) excited states (i.e., CIS method). The basis set used is of 6-31G quality. All excited states modeled are of the singlet type. The CIS calculations in the present QMC implementation have been performed with the help of the GAUSSIAN 94 program.[53] We are aware of the fact that the chosen setup for H_{el} is insufficient for a quantitative reproduction of the excited-state properties of the two benzene isomers. Spectroscopic measurements,[4,33−35] as well as previous calculations[24−31] with state-of-the-art Hamiltonians H_{el}, have shown that intervalence and Rydberg transitions occur in the same low-energy window. The 6-31G basis

is too small to describe Rydberg states. The limitations of the CIS method have been studied by several authors.[25,26,28,29] The present electronic setup is however sufficient to discuss and to understand a physical effect that has been neglected in previous ab initio studies of the excited-state properties of benzene.

In analogy to our recent PIMC−ab initio simulations of ground-state properties of benzene[41,42,47] we have adopted an accurate model potential $V(\mathbf{R})$ to evaluate the ground-state Born−Oppenheimer surface.[54] In connection with vertical FC transitions, it suffices to construct the ground-state PES of the respective molecule. The analysis of non-FC effects would require the evaluation of a separate BO surface for each excited state. In two of our recent PIMC−ab initio papers,[46,55] we have developed some experience in analyzing the excited-state properties of molecules under consideration of the nuclear degrees of freedom. In these contributions, we could explain an unexpected theoretical result. CBO calculations of the excited states of ethylene have shown that improvements in the setup of H_{el} are not necessarily accompanied by theoretical results which are closer to experiment.[46] The physical origin of such a supposed paradox will be reconsidered in the present benzene study.

The PIMC−ab initio CIS approach developed by the present authors is a two-step formalism. In the first PIMC step, we consider the quantum and thermal degrees of freedom of the C_6H_6 and C_6D_6 nuclei moving on the $V(\mathbf{R})$ based PES. In this step, we generate molecular (ground state) configurations which are populated at a given temperature and for given atomic masses. In the second ab initio step, these nuclear configurations are used as input for CIS calculations. On the basis of our previous computational experience,[42,45−47] we have adopted 6000 different molecular configurations in the ab initio CIS step of our two-step approach.

Temperatures of 50 and 750 K have been considered in the QMC simulations of the two benzene isomers. $T = 50$ K implies that the nuclear degrees of freedom are of the bare quantum mechanical zero-point type. In recent QMC studies of hydrocarbons[42,45−47] and fullerenes[56,57] we have emphasized that the nuclear fluctuations up to room temperature (RT) are quantum driven. $T = 750$ K has been chosen to model the excited-state properties of C_6H_6 and C_6D_6 under conditions where the classical thermal nuclear degrees of freedom are no longer negligible. We accept that such high-temperature simulations are of only limited value under bare experimental considerations. They have been chosen to model a second theoretical boundary.

We have given this rather detailed introduction in order to illuminate the experimental and theoretical background of the present research. To reemphasize, electronic excitation spectra of molecules are ideal subjects to analyze the coupling between electronic and nuclear degrees of freedom (key words: vibrational broadening of electronic transitions, vibrational borrowing,[4,58,59] nonzero intensities of symmetry-forbidden states). Benzene has been one of the first examples where these phenomena have been detected in spectroscopic measurements.[4,33−35] Despite these challenging experimental observations one has to confess that the published computational ab initio studies of the excited states of benzene make use of the CBO approximation. It seems that previous theoretical efforts have been directed prevailingly toward improvements in the definition of H_{el}. At the same time, a well-known physical effect has been neglected in recent ab initio studies of the excited-state properties of benzene.

The organization of the present work is as follows. In section II, we explain the theoretical background of the PIMC−ab initio approach employed. A concise description of the computational conditions is given in section III. In the next one, we discuss the spatial uncertainty of the benzene nuclei. Furthermore, we comment on the influence of anharmonicities in the nuclear potential $V(\mathbf{R})$ on the bond lengths r_{cc} and r_{cx} (X = H, D) in thermal equilibrium. The comparison of thermally averaged r_g, α_g coordinates (α sybolizes a bondangle) with the r_e, α_e coordinates at the PES minimum (i.e., $\mathbf{R_o}$ structure) visualizes the inherent problem of CBO calculations which make use of $\mathbf{R_o}$ coordinates. In section V, we correlate the excited-state properties of C_6H_6 and C_6D_6 as derived by QMC simulations of the ABO type with simple CBO results. The article ends with a short resume.

II. Theoretical Background

In this section, we summarize the basic principles of our PIMC−ab initio implementation in a setup which allows the simulation of molecular electronic excited states under the conditions of thermal equilibrium. Detailed descriptions of the PIMC technique can be found in the literature.[36−40] Path integral expressions for molecular problems with a nuclear and an electronic Hamiltonian have been derived by Cao and Berne.[60] The theoretical problems, which can occur in such systems with fast and slow motions have been commented on in detail in ref 60; see below. In the first PIMC step of our two-step approach we have simulated the thermal and quantum degrees of freedom of the C_6H_6 and C_6D_6 nuclei. Each nucleus i ($i = 1$ to 6 for the C atoms, $i = 7$ to 12 for the H (D) atoms) has been treated as a quantum particle. The total number of atoms (= 12) is denoted by n. The key principles of the PIMC method are well-known. The isomorphism between a single quantum particle (here each nucleus of C_6H_6 or C_6D_6) and a cyclic chain of N classical particles (= beads) renders possible the use of classical MC techniques to derive the finite-temperature properties of the original quantum system. The Metropolis method has been employed to evaluate the $T \neq 0$ K properties of the two benzene isomers.[61] Test calculations have shown that the accuracy of this simple sampling technique is sufficient.[62] Thus is has not been necessary to use improved sampling methods such as staging MC or Fourier PIMC.[63,64]

Let us start with the definition of the nuclear Hamiltonian H_{nuc}

$$H_{nuc} = -\sum_{i=1}^{n}\left[\frac{\hbar^2}{2m_i}\left(\frac{\partial^2}{\partial r_{ix}^{\,2}} + \frac{\partial^2}{\partial r_{iy}^{\,2}} + \frac{\partial^2}{\partial r_{iz}^{\,2}}\right)\right] + V(\mathbf{R}) \quad (1)$$

The summation in eq 1 is over all C_6H_6 (C_6D_6) nuclei. $\hbar$ denotes the Planck constant. The $r_{ix(y,z)}$ describe the Cartesian coordinates of each nucleus i; they define the components of three-dimensional atomic position vectors $\mathbf{r}_i$. With the help of the $\mathbf{r}_i$ it is possible to express the vector $\mathbf{R}$. We have $\mathbf{R} = (\mathbf{r}_1,\mathbf{r}_2 \ldots \mathbf{r}_n)$. The m_i in eq 1 abbreviate the masses confined to the atoms i. $V(\mathbf{R})$ stands for the potential acting on the nuclei. For the present QMC simulations, we have employed the model potential described in ref 54; see also the improvements suggested in our recent PIMC−ab initio study of benzene.[42]

For the second computational step of the suggested PIMC−ab initio formalism, we have adopted the CI routine of the GAUSSIAN 94 package. The present combination of two methods implies to correlate $V(\mathbf{R})$ of the first PIMC step with electronic energies emerging from ab initio calculations. Recent ground state simulations of benzene have shown that both computational methods yield BO surfaces which coincide

sufficiently in the neighborhood of the minimum.[42,47] As a matter of fact only small violations from self-consistency have to be expected. We refer to some of our previous QMC works.[42,46,47]

The partition function Z for the quantum system is defined in eq 2; Z is given by the trace of the statistical density matrix $\rho(\mathbf{R},\mathbf{R}';\beta)$

$$Z = \mathrm{tr}[\rho(\mathbf{R},\mathbf{R}';\beta)] = \mathrm{tr}[\exp(-\beta H_{\mathrm{nuc}})] \tag{2}$$

The parameter β reads $\beta = (k_B T)^{-1}$ with k_B symbolizing the Boltzmann constant. The definition of the partition function Z in terms of the statistical density matrix is a central element of the PIMC approach. It leads to a peculiarity in the computational results which should be mentioned. PIMC simulations produce mixed ensemble states for the nuclear problem which cannot be described by a single wave function. This superposition of bare quantum states has certain implications for PIMC based intensities ${}^{\mathrm{PI}}\bar{f}_{\mathrm{osc}}$ of electronic transitions. In section V, we come back to this point. Central matter of concern of the present research is the comparison of singlet transition energies E_T and oscillator strengths f_{osc} of C_6H_6 and C_6D_6 in the CBO approximation with ensemble averaged QMC quantities ${}^{\mathrm{PI}}\bar{E}_T$ and ${}^{\mathrm{PI}}\bar{f}_{\mathrm{osc}}$. To derive the ensemble averages 6000 different molecular configurations (i.e., geometries) have been taken into account. The population of these nuclear configurations follows a canonical ensemble statistics. On the basis of our introductory remarks, it is now possible to relate the excited states properties of the two benzene isomers as derived in the present ABO picture to the much simpler CBO findings. For this purpose, we define the total molecular wave function Ψ by the product of the electronic wave function $\Psi_{\mathrm{el}}(\mathbf{r}_{\mathrm{el}},\mathbf{R})$, see above, and the vibrational wave function $\Psi_v(\mathbf{R})$. v symbolizes the vibrational quantum number. In eq 3, we give the most general expression for a spectroscopic transition moment between initial and final states Ψ'' and Ψ'[65]

$$M_{\mathrm{el},v',v''} = \int d\mathbf{R} \int d\mathbf{r}_{\mathrm{el}} \Psi'^{*}(\mathbf{D}_{\mathrm{el}} + \mathbf{D}_{\mathrm{n}})\Psi'' \tag{3}$$

$\mathbf{D}_{\mathrm{el}}$ and $\mathbf{D}_{\mathrm{n}}$ abbreviate the electronic and nuclear contributions to the overall dipole operator $\mathbf{D}$. Insertion of the product wave function $\Psi = \Psi_v(\mathbf{R})\Psi_{\mathrm{el}}(\mathbf{r}_{\mathrm{el}},\mathbf{R})$ into eq 3 and consideration of the orthogonality between the initial and the final electronic states leads to

$$M_{\mathrm{el},v',v''} = \int d\mathbf{R}\Psi_{v'}{}^{*}(\mathbf{R})\Psi_{v''}(\mathbf{R}) \int d\mathbf{r}_{\mathrm{el}}\Psi_{\mathrm{el}}{}'^{*}(\mathbf{r}_{\mathrm{el}},\mathbf{R})\mathbf{D}_{\mathrm{el}}\Psi_{\mathrm{el}}{}''(\mathbf{r}_{\mathrm{el}},\mathbf{R}) \tag{4}$$

The standard method to evaluate the transition moments of eq 4 is based on the following approximation.[65] One assumes that, for any given nuclear configuration $\mathbf{R}$, the electronic dipole moment is an only slowly varying function of $\mathbf{R}$. This a priori assumption forms the basis of the CBO approximation. We derive an electronic transition moment where the set of vectors $\mathbf{R}$ has been replaced by a single vector, i.e., the vector $\mathbf{R}_o$. Remember that $\mathbf{R}_o$ maps the nuclear coordinates at the minimum of the BO surface. With this approximation we observe eqs 5 and 6

$$M_{\mathrm{el},v',v''} \approx \mathrm{M}(\mathbf{R}_0) \int d\mathbf{R}\Psi_{v'}{}^{*}(\mathbf{R})\Psi_{v''}(\mathbf{R}) \tag{5}$$

$$\mathrm{M}(\mathbf{R}_0) = \int d\mathbf{r}_{\mathrm{el}}\Psi_{\mathrm{el}}{}'^{*}(\mathbf{r}_{\mathrm{el}},\mathbf{R}_0)\mathbf{D}_{\mathrm{el}}\Psi_{\mathrm{el}}{}''(\mathbf{r}_{\mathrm{el}},\mathbf{R}_0) \tag{6}$$

With the help of the last relation, it is easy to recognize that it is the point symmetry at the minimum of the PES which determines whether an electronic transition is dipole-allowed in the CBO hierarchy. The vertical transition energies E_T in this theoretical framework are given by the difference between two electronic energies which have been calculated for the $\mathbf{R}_0$ geometry. Note that the choice to adopt identical molecular geometries in the two electronic states under consideration is in line with the FC principle. Capabilities and weaknesses of the CBO method to evaluate the excited state properties of molecules can be described as follows. (i) The CBO picture implies a highly simplified description of the electronic problem (eq 6). (ii) In the framework of the FC principle, it is, at least in principle, possible to treat the vibrational structure of electronic transitions accurately. Note that the transition moment depends on the vibrational quantum numbers v' and v''. (iii) Inspection of the literature, however, shows that this degree of freedom of the classical approach is only seldom considered. In the majority of excited-state calculation of molecules,[23−31] eq 6 is used for the comparison between measured and theoretically calculated transition intensities. This choice is easy to explain: the evaluation of vibrational wave functions $\Psi_v(\mathbf{R})$ of complex polyatomic molecules beyond the simple harmonic approximation is still a nontrivial task.[11−14,66,67]

Now let us explain the theoretical basis of the ABO approach. (i) This method renders possible a more accurate treatment of the electronic degrees of freedom. At the same time it requires simplifications in the vibrational part of the molecular Hamiltonian. (ii) In the present implementation, we assume that both electronic states (i.e., initial and final state) can be described by the same set of vibrational wave functions. This simplification prevents quantitative reproductions of the vibrational structure of electronic transitions. It follows from the ensemble character of PIMC solutions. See the discussion in connection with eq 2. Because the majority of excited-state calculations of molecules has been restricted to the $\mathrm{M}(\mathbf{R}_0)$ term in eq 6, the present simplification in the vibrational problem should be acceptable. (iii) To emphasize, it is the large advantage of the present ABO implementation that the nuclear coordinate (i.e., $\mathbf{R}$) dependence of the electronic transition moment is explicitly taken into account. General definitions for the ensemble averaged transition moment $\bar{M}_{\mathrm{el}}$ and transition energy $\bar{E}_T$ can be found in eqs 7 and 8. Note that specific vibrational quantum numbers v' and v'' do not occur in the thermal mean value of the transition moment which has been derived with the help of a multidimensional reflection principle

$$\bar{\mathrm{M}}_{\mathrm{el}} = \int d\mathbf{R}P(\mathbf{R}) \int d\mathbf{r}_{\mathrm{el}}\Psi_{\mathrm{el}}{}'^{*}(\mathbf{r}_{\mathrm{el}},\mathbf{R})\mathbf{D}_{\mathrm{el}}\Psi_{\mathrm{el}}{}''(\mathbf{r}_{\mathrm{el}},\mathbf{R}) \tag{7}$$

$$\bar{E}_T = \int d\mathbf{R}P(\mathbf{R})E_T(\mathbf{R}) \tag{8}$$

The function $P(\mathbf{R})$ in the two equations defines the statistical weight of the different nuclear configurations. $P(\mathbf{R})$ is given by

$$P(\mathbf{R}) = Z^{-1}\sum_v [-\beta E_v(\mathbf{R})] \times |\Psi_v(\mathbf{R})|^2 \tag{9}$$

The summation is over all vibrational states v. E_v is the v'th eigenvalue of the nuclear Hamiltonian H_{nuc}. The partition function Z in eq 9 has been introduced in eq 2. The last relation explains that PIMC simulations produce mixed states which correspond to a superposition of pure quantum states. For $T = 0$ K, $P(\mathbf{R})$ is exclusively determined by the square of the ground-state nuclear wave function. Equations 7 and 8 can be considered as general prescriptions for the evaluation of thermal expectation values. In eqs 10 and 11, we give the path integral estimator

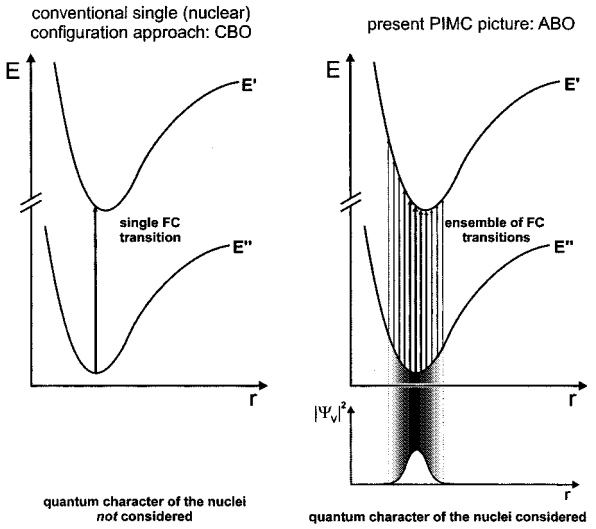

Figure 1. Schematic diagram symbolizing the difference between conventional CBO calculations of electronic excitation processes in molecules (lhs.) and the present ABO approach (rhs.) We have chosen a diatomic example with only one nuclear degree of freedom r which denotes the internuclear separation. The E'' and E' symbolize energies of the initial and final electronic states. The Franck−Condon principle has been assumed in both theoretical degrees of sophistication. In the ABO description an ensemble of FC transitions is evaluated. Their weight is given by the square of the nuclear wave function $\Psi_v \equiv \Psi_v(\mathbf{R})$; bottom diagram on the rhs. of the figure ($T = 0$ K).

expressions for the ensemble averaged transition moment and transition energy

$$^{PI}\bar{M}_{el} = 1/(NQ)\sum_j \int d\mathbf{r}_{el}\Psi_{el}'^*(\mathbf{r}_{el},\mathbf{R}_j)\mathbf{D}_{el}\Psi_{el}''(\mathbf{r}_{el},\mathbf{R}_j) \quad (10)$$

$$^{PI}\bar{E}_T = 1/(NQ)\sum_j E_T(\mathbf{R}_j) \quad (11)$$

The index j in the two formulas refers to the j'th nuclear configuration generated in the MC step of the present two-step approach. j covers the values from $j = 1$ to $j = NQ$ with N abbreviating the number of time-slices (beads) and Q the number of MC steps. The label PI has been added to the quantities in eqs 10 and 11 in order to emphasize the PI origin of the ensemble averages. The present PI expressions coincide with formulas derived in ref 60. In this work, it has been shown that the formulas are valid if none of the electronically excited states of the molecule considered is thermally excited. This condition is clearly fulfilled for the two benzene isomers studied. The lowest excited singlet states in both π molecues are several eV above the electronic ground state; see section V. It is self-explanatory that the number of nuclear configurations adopted in the ab initio ensemble averaging is smaller than the upper boundary defined in eqs 10 and 11. In section III, we come back to this point.

Figure 1 has been prepared to visualize schematically (for a one-dimensional model potential) the difference between CBO calculations of electronic transitions and the present ABO approach. To reemphasize; in the CBO approximation only a single FC transition between the initial and final electronic state is calculated. The $\mathbf{R}_0$ geometry adopted in the majority of calculations defines a vibrationless model structure not realized experimentally. The intensity of an electronic dipole transition is controlled by the point symmetry of the $\mathbf{R}_0$ configuration; lhs. of Figure 1. The present ABO approach, rhs. of Figure 1, takes into account the quantum and thermal degrees of freedom of the nuclei. In this theoretical scheme, we calculate a manifold of vertical FC transitions, i.e., a multidimensional distribution function, from molecular configurations with weighting factors which are determined by a canonical ensemble statistics. Note that the "symmetry constraints" operative for the high point symmetry at the minimum of the BO surface are attenuated in ABO simulations. The nuclear configurations generated in thermal equilibrium are lower in symmetry than the configuration at the minimum of the PES.

At the end of the theory section let us come back to another inherent problem of the CBO model. Remember that this scheme is based on two severe simplifications. (i) It neglects the wave packet character of the nuclear wave function. This is the bottleneck of any single configuration approach. (ii) It makes use of vibrationless $\mathbf{R}_0$ coordinates. The bond lengths and bondangles of the $\mathbf{R}_0$ structure have been symbolized by r_e, α_e. A possible way to avoid at least the errors of approximation (ii) in single-configuration studies might be the adoption of r_g, α_g coordinates, i.e., bond lengths and bondangles in thermal equilibrium. The evaluation of thermally averaged geometrical parameters of molecules is a trivial procedure in QMC studies. It occurs in the first PIMC step. To derive thermally averaged configurations described by the vector $^{PI}\bar{R}$, we make use of eq 12

$$^{PI}\bar{R} = \sum_m P(\mathbf{R}_m)\mathbf{R}_m \quad (12)$$

$P(\mathbf{R}_m)$ is the above-mentioned nuclear weight function. In contrast to the post PIMC calculations of electronic excitation energies and oscillator strengths (i.e., CIS approach) in the second computational step of the present QMC approach, the thermally averaged coordinates $^{PI}\bar{R}$ are evaluated in the first PIMC step. Thus, it is possible to choose a number of configurations in eq 12 which is much larger than the configuration count of 6000 employed in the ab initio averaging. In section V, the symbol E_T* will be used to denote a second set of electronic excitation energies of the single configuration type. The oscillator strengths associated to the E_T* energies are denoted by f_{osc}*. But in contrast to the E_T set, the E_T* numbers have been derived for a D_{6h} structure of C_6H_6 (C_6D_6) which is defined by r_g bond lengths. An identity $^{PI}\bar{E}_T = E_T$* and, even more important $^{PI}\bar{f}_{osc} = f_{osc}$*, would indicate a vanishing wave packet character of the nuclear wave function as far as excited-state properties of molecules are concerned. In this context, let us mention the review article of Kuchitsu where internal coordinates of the r_g, α_g type have been related to the hypothetical r_e, α_e set.[68]

III. Computational Conditions

In the following, we give a short description of the computational conditions adopted. The number of beads N as well as the number of QMC steps Q has been chosen on the basis of our previous QMC simulations of hydrocarbons.[42,45−47] The number of beads in the PIMC runs has been fixed to $N \times T = 6000$ K. With this criterion it has been possible to derive expectation values of H_{nuc} with an accuracy better than 0.5%. For a detailed discussion of the MC error bars, we refer to ref 62. Note, however, that such nuclear quantities are not the main topic of the present analysis. Detailed discussions of nuclear expectation values of benzene in thermal equilibrium can be found in refs 42,47. The number of nuclear configurations generated in the PIMC step lies between 4×10^5 and 6×10^6. From these long QMC trajectories, 6000 nuclear configurations

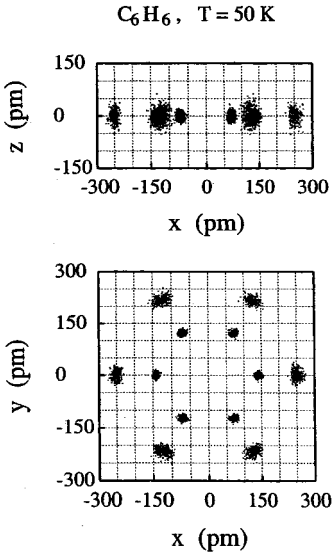

Figure 2. Probability distribution function (pdf) of the C_6H_6 nuclei at $T = 50$ K. The distribution has been derived by PIMC simulations with nuclei moving on the $V(\mathbf{R})$ based PES. Top diagram: pdf perpendicular to the benzene plane; bottom diagram: pdf onto the horizontal molecular plane.

have been chosen for the second ab initio CIS step. Here, constant spacings between the members of the long PIMC trajectories have been adopted. The configuration count in the second ab initio step is a fair compromise between intended accuracy of the QMC results on one hand and computational constraints, on the other. Test calculations have shown that the error bars of the PIMC simulations are not enlarged in the second ab initio step.

It has been mentioned in the Introduction that we have adopted a model potential $V(\mathbf{R})$[54] to derive the ground-state BO surface of benzene in the PIMC step. The parameters of $V(\mathbf{R})$ have been chosen to reproduce geometries and vibrational wavenumbers of hydrocarbons. The CIS calculations have been performed with the help of the GAUSSIAN 94 program.[53] Capabilities and the failures of this CI method in combination with the adopted 6−31 G basis have been commented on in detail.[22,26,28,29] The CIS ensemble averagings have been performed on an AMD Athlon 800 computer operating under Linux.

IV. Spatial Nuclear Delocalization and Geometrical Parameters in Thermal Equilibrium

The comparative discussion of the ABO quantities $^{PI}\bar{E}_T$, $^{PI}\bar{f}_{osc}$, and the CBO data E_T, f_{osc} of C_6H_6 and C_6D_6 in the next section is largely simplified if we first touch upon the spatial uncertainty of the nuclei as well as the geometrical parameters of the two π systems at the minimum of the BO surface and in thermal equilibrium. A detailed presentation of these results has been given in one of our recent contributions where we have determined NMR shieldings of benzene by means of PIMC−ab initio simulations.[47] In Figure 2 we have portrayed two-dimensional (2D) projections of the probability distribution function (pdf) of the C_6H_6 nuclei. The temperature considered amounts to 50 K. This choice guarantees that the nuclear fluctuations are of the quantum mechanical zero-point type. The following conclusions can be deduced from Figure 2. (i) Both types of C_6H_6 nuclei are strongly delocalized. (ii) The nuclear delocalization of the light hydrogens is however somewhat larger than the delocalization of the heavy carbons, a grading which has been expected for nuclear quantum fluctuations. (iii) The planar D_{6h} configuration of benzene is an exception in thermal equilibrium. (iv) The observed wave packet character of the nuclear wave function of C_6H_6, as well as of C_6D_6, might be an obstacle for the derivation of "exact" excitation energies and intensities in the framework of the CBO approach even if H_{el} is of state-of-the-art quality.

TABLE 1: Geometrical Parameters of C_6H_6 (top part) and C_6D_6 (bottom part)[a]

origin of the data					
C_6H_6	X = H	r_{CC}	r_{CX}	α_{CCC}	α_{CCX}
minimum PES		140.7	109.2	120.0	120.0
PIMC 50 K		141.5	111.1	119.7	119.4
PIMC 750 K		142.0	111.3	119.2	119.1
experiment r_g, α_g		139.7	108.4	120.0	120.0
origin of the data					
C_6D_6	X = D	r_{CC}	r_{CX}	α_{CCC}	α_{CCX}
PIMC 50 K		141.5	110.6	119.7	119.5
PIMC 750 K		142.0	110.8	119.2	119.2

[a] In the first line of the C_6H_6 collection we have given the vibrationless r_e, α_e coordinates at the minimum of the $V(\mathbf{R})$ based PES. The remaining theoretical results refer to thermal r_g, α_g values derived by PIMC simulations at $T = 50$ and 750 K. In the bottom line of the C_6H_6 collection experimental quantities have been given. They have been taken from ref 4. All bondlengths in pm, all bondangles in degrees.

After having mentioned the nuclear delocalization in C_6H_6 let us consider the differences between the internal coordinates of C_6H_6 and C_6D_6 at the minimum of the PES and in thermal equilibrium. A collection of theoretically determined C_6H_6 and C_6D_6 bond lengths and angles has been given in Table 1. The theoretical C_6H_6 results have been supplemented by experimental diffraction data.[4] We find that the bonds in C_6H_6 and C_6D_6 are strongly elongated under the influence of the nuclear degrees of freedom. These effects are particularly large for the CH and CD bonds. For C_6H_6, we predict thermal CH elongations between 1.9 pm ($T = 50$ K) and 2.1 pm ($T = 750$ K). In C_6D_6, the differences between the r_g and r_e coordinates are found between 1.4 and 1.6 pm. The bond length enhancement for the CC bonds due to the anharmonicities in the potential $V(\mathbf{R})$ is smaller. At $T = 50$ K the CC bonds of both π systems are elongated by 0.8 pm under the influence of the nuclear degrees of freedom. At $T = 750$ K the r_g and r_e parameters differ by 1.3 pm. In our recent C_2H_4 analysis, we have shown that the calculated differences between the r_g and r_e lengths are close to experiment.[45] Such a comparison between two sets of experimental length parameters has not been possible for the benzene molecule where experimentally deduced r_e coordinates are missing.

At the end of this section let us emphasize a peculiarity in the bondangles α_{CCC} and α_{CCX} (X = H, D) in thermal equilibrium. The three bondangles per CCXC fragment differ from 360°. Note that only an angular sum of 360° is compatible with a planar benzene structure. We interpret the observed "angular defect" as an indicator for the wave packet character of the nuclear wave function. It has its origin in nonplanar molecular configurations that are generated under the influence of the spatial fluctuations of the atoms; see Figure 2. We have demonstrated that the combined influence of anharmonicities in the nuclear potential $V(\mathbf{R})$ and the strong quantum delocalization of the C_6H_6 and C_6D_6 nuclei lead to internal coordinates r_g, α_g which differ from the r_e, α_e set (= $\mathbf{R}_0$ configuration). The implications for calculated excited-state properties which follow from these differences are discussed in the following section.

TABLE 2: Electronic Excitation Energies (singlet transitions) E_T, $^{PI}\bar{E}_T$ and Oscillator Strengths f_{osc}, $^{PI}\bar{f}_{osc}$ of C_6H_6 According to CIS Calculations in a 6−31 G Basis Set[a]

		minimum PES		PIMC 50 K		PIMC 750 K		experiment	
state	type of the transition	E_T	f_{osc}	$\bar{E}_T$	$^{PI}\bar{f}_{osc}$	$\bar{E}_T$	$^{PI}\bar{f}_{osc}$	$\bar{E}_T$	$\bar{f}_{osc}$
$^1B_{2u}$	$\pi \rightarrow \pi^*$	6.32	−	6.16 (0.18)	0.018 (0.033)	5.98 (0.15)	0.030 (0.042)	4.9	0.001
$^1B_{1u}$	$\pi \rightarrow \pi^*$	6.53	−	6.31 (0.18)	0.031 (0.022)	6.16 (0.24)	0.038 (0.029)	6.2	0.090
$^1E_{1u}$	$\pi \rightarrow \pi^*$	8.53	1.144	8.14 (0.22) 8.28 (0.20)	0.726 (0.280) 0.811 (0.212)	7.88 (0.31) 8.06 (0.28)	0.616 (0.261) 0.694 (0.208)	7.0	0.900
$^1A_{2u}$	$\sigma \rightarrow \pi^*$	9.37	−	8.65 (0.23)	0.278 (0.300)	8.47 (0.28)	0.283 (0.271)		
$^1E_{1g}$	$\pi \rightarrow \sigma^*$	9.50	−	8.95 (0.22) 9.17 (0.20)	0.103 (0.170) 0.055 (0.065)	8.80 (0.25) 9.03 (0.23)	0.114 (0.161) 0.073 (0.081)		
$^1A_{1u}$	$\sigma \rightarrow \pi^*$	9.65	−	9.34 (0.19)	0.049 (0.042)	9.24 (0.23)	0.065 (0.067)		

[a] In the table the results for the eight lowest singlet states have been given. The first set of numbers (E_T, f_{osc}) has been derived for the D_{6h} structure of C_6H_6 at the $V(\mathbf{R})$ based minimum (CBO Results). All irreducible representations on the lhs. Refer to this symmetry. The second (third) set of numbers refers to a PIMC ensemble averaging at $T = 50$ (750) K. The numbers in parantheses denote the standard deviation σ_i of the $^{PI}\bar{E}_T$ and $^{PI}\bar{f}_{osc}$ derived within the ensemble of 6000 different nuclear configurations. Experimental results have been given on the extreme right.[32,35] All transition energies are given in eV.

V. Excited State Properties

In this section, we discuss the excited singlet states of C_6H_6 and C_6D_6 as derived by PIMC−ab initio CIS simulations. We have already mentioned that the technical setup in the design of H_{el} prevents a quantitative reproduction of the measured optical spectrum of the two benzene isomers. Despite these technical limitations, we are convinced that our QMC approach offers new insight into physical effects accompanying the electronic transitions in the two benzene isomers. Three singlet transitions arising from the HOMO−LUMO manifold have been identified unambiguously in the optical spectrum of C_6H_6. Their Franck−Condon maxima occur at 4.9, 6.2 and 7.0 eV.[4,22] The absorptions are due to transitions into $^1B_{2u}$, $^1B_{1u}$ and $^1E_{1u}$ states (D_{6h} representations). Only the transition to the $^1E_{1u}$ state is dipole-allowed under strict D_{6h} conditions. Nevertheless, one observes nonvanishing oscillator strengths for the first two singlet transitions. Values of 0.001 and 0.09 have been reported in the literature.[32,35] The measured oscillator strength for the $^1E_{1u}$ transition amounts to 0.90.[32,35]

In Table 2 , we have summarized transition energies E_T and intensities f_{osc} of C_6H_6 for the D_{6h} minimum of the PES as well as the ensemble averages $^{PI}\bar{E}_T$ and $^{PI}\bar{f}_{osc}$. The temperatures considered in the two QMC runs amount to 50 and 750 K. The theoretical analysis covers the eight lowest singlet states of C_6H_6, i.e., an array larger than the number of singlet valence states which have been identified spectroscopically. The decision to consider such a rather large set of excited singlet states can be explained as follows. To understand the influence of the nuclear degrees of freedom on electronic excitation processes, a sufficiently large array of electronic transitions is indispensable. The nature of "vibronic coupling" and "borrowing" becomes clear only if a larger number of excitations is dipole-forbidden under D_{6h} symmetry and if at least one excitation is dipole-allowed at the minimum of the PES. On the rhs. of Table 2, we have quoted the experimental transition energies and oscillator strengths of C_6H_6.[4,32,35] The material of the table has been supplemented by the graphical representation in Figure 3. Here, we have displayed the ensemble averages $^{PI}\bar{E}_T$ and $^{PI}\bar{f}_{osc}$ (top diagram) and the distribution functions of FC transitions (bottom diagram) calculated for the eight lowest singlet transitions in C_6H_6. The distribution functions show the spreading of the FC transitions due to the wave packet character of the atomic nuclei. But as explained in the theory section, such a PIMC based distribution function does not provide a quantitative description of the vibrational structure of electronic spectra. The C_6D_6 results can be found in Table 3 and Figure 4. The QMC simulations demonstrate clearly that excited-state calculations of molecules

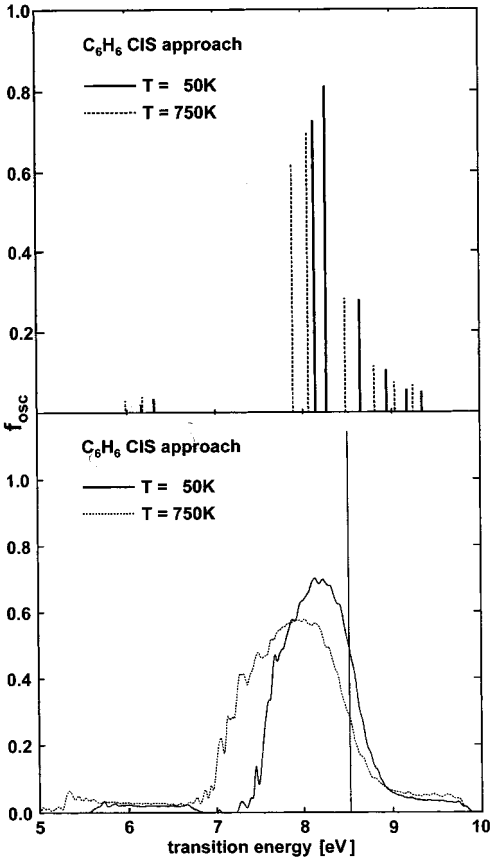

Figure 3. Top part: Histogram with the eight lowest singlet transition energies $^{PI}\bar{E}_T$ (in eV) and intensities $^{PI}\bar{f}_{osc}$ of C_6H_6 at $T = 50$ K (full lines) and 750 K (broken lines). Bottom part: Distribution function of the eight lowest singlet transitions in C_6H_6 at $T = 50$ K (full curve) and 750 K (broken curve). The PIMC−ab initio CI results have been derived via an ensemble averaging covering 6000 different C_6H_6 geometries. The first dipole-allowed $\pi \rightarrow \pi^*$ transition to the $^1E_{1u}$ state at the PES minimum has been indicated in the bottom diagram (full vertical line at $E_T = 8.53$ eV, $f_{osc} = 1.144$).

on the basis of a single nuclear configuration (i.e., restriction to one benzene geometry with D_{6h} symmetry) should be considered as a highly idealized model approach only. Have a look at the bottom diagram in Figure 3. The plot shows that the simple CBO approach leads to a single δ-shaped transition E_T with $f_{osc} \neq 0$ ($E_T = 8.53$ eV). The PIMC−ab initio approach yields a distribution function (lower plot in the figure) which covers several eV. The relative intensities of the ensemble averaged transitions are in sufficient agreement with experi-

TABLE 3: Electronic Excitation Energies of C_6D_6[a]

state	type of the transition	minimum PES		PIMC 50 K		PIMC 750 K	
		E_T	f_{osc}	${}^{PI}\bar{E}_T$	${}^{PI}\bar{f}_{osc}$	${}^{PI}\bar{E}_T$	${}^{PI}\bar{f}_{osc}$
$^1B_{2u}$	$\pi \rightarrow \pi^*$	6.32	–	6.19 (0.17)	0.017 (0.033)	6.00 (0.25)	0.028 (0.040)
$^1B_{1u}$	$\pi \rightarrow \pi^*$	6.53	–	6.33 (0.18)	0.030 (0.022)	6.18 (0.24)	0.039 (0.029)
$^1E_{1u}$	$\pi \rightarrow \pi^*$	8.53	1.144	8.20 (0.21) 8.33 (0.19)	0.774 (0.278) 0.846 (0.224)	7.91 (0.30) 8.08 (0.28)	0.643 (0.255) 0.716 (0.200)
$^1A_{2u}$	$\sigma \rightarrow \pi^*$	9.37	–	8.70 (0.22)	0.275 (0.314)	8.52 (0.27)	0.275 (0.268)
$^1E_{1g}$	$\pi \rightarrow \sigma^*$	9.50	–	9.01 (0.20) 9.23 (0.18)	0.080 (0.154) 0.044 (0.051)	8.86 (0.29) 9.08 (0.22)	0.097 (0.142) 0.067 (0.071)
$^1A_{1u}$	$\sigma \rightarrow \pi^*$	9.65	–	9.34 (0.18)	0.039 (0.044)	9.27 (0.21)	0.061 (0.062)

[a] See legend to Table 2. Note that the E_T and f_{osc} (first set of numbers) coincide with the C_6H_6 results of Table 2.

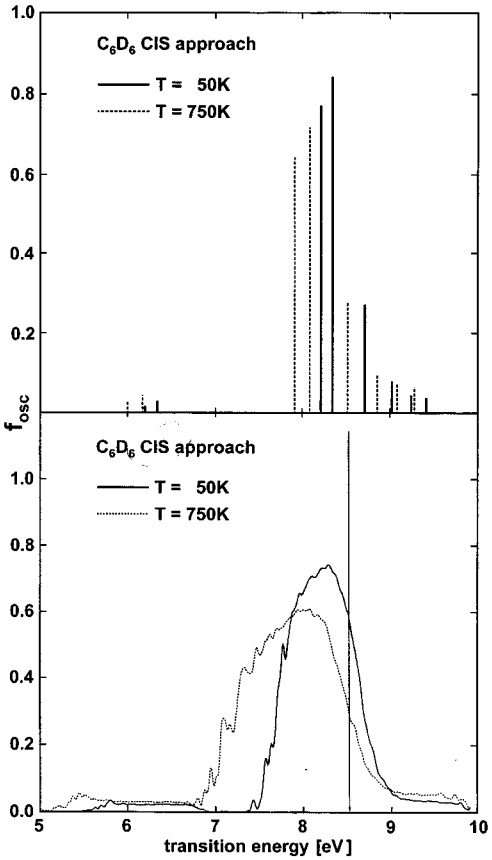

Figure 4. Histogram defined by the eight lowest singlet transition energies ${}^{PI}\bar{E}_T$ and intensities ${}^{PI}\bar{f}_{osc}$ (top diagram) as well as the associated distribution functions (bottom diagram) of C_6D_6. See legend to Figure 3.

ment;[32,34,35] see also below. Even the width of the intensity distributions is in qualitative agreement with experiment. The experimental width of the dipole-forbidden $^1B_{2u}$ transition amounts to roughly 0.83 eV;[35] the present theory yields 1.3 eV. For the first dipole allowed $^1E_{1u}$ transition, we observe experimental[34] and calculated width parameters of 1.0 and 1.7 eV. The comparison between experimental and theoretical distribution functions shows that anharmonicities are somewhat overestimated by the model potential $V(\mathbf{R})$ which has been used in the MC step.

The nuclear degrees of freedom in C_6H_6 and C_6D_6 lead to singlet transitions $E_T(\mathbf{R})$, ${}^{PI}\bar{E}_T$ which are all dipole-allowed; i.e., all $f_{osc}(\mathbf{R})$, ${}^{PI}\bar{f}_{osc}$ evaluated are larger than zero. The calculated oscillator strengths ${}^{PI}\bar{f}_{osc}$ for the transitions to the $^1B_{2u}$ and $^1B_{1u}$ states reproduce the experimental values at least qualitatively. The calculated sum of the two ${}^{PI}\bar{f}_{osc}$ numbers of 0.059 ($T = 50$ K) should be compared with the experimental estimate of 0.091. To understand the physical meaning of the ${}^{PI}\bar{E}_T$ and ${}^{PI}\bar{f}_{osc}$ in Tables 2 and 3, it is necessary to reemphasize the ensemble character of the present QMC results. The Cartesian displacements of the nuclei in the PIMC step guarantee that all vibrational modes contribute to the ensemble averaged results. At the same time these ensemble results are incompatible with a mode-selective coupling of vibrations to electronic states, a coupling mechanism discussed by Herzberg and other authors.[4]

The results in Tables 2 and 3 as well as the information provided by Figures 3 and 4 demonstrate that the nuclear degrees of freedom have a strong influence both on the transition energies ${}^{PI}\bar{E}_T$ and on the oscillator strengths ${}^{PI}\bar{f}_{osc}$. A short comment on the second quantity has been given above; but see below for further details. We start with a comparative discussion of the E_T and ${}^{PI}\bar{E}_T$ numbers. In contrast to the T- and isotope-independent E_T elements, we evaluate ensemble averages ${}^{PI}\bar{E}_T$ with a sizable T- and isotope-dependence. The inequality ${}^{PI}\bar{E}_T < E_T$ is valid for all singlet transitions studied. The shift parameter $\Delta E_T = E_T - {}^{PI}\bar{E}_T$ is enhanced with increasing temperature and reduced isotope mass. Both factors support the coupling between nuclear and electronic degrees of freedom.[42,45,46] For the $T = 50$ K simulation of C_6H_6, we predict ΔE_T elements between 0.16 and 0.72 eV. $T = 750$ K leads to shift parameters ΔE_T between 0.37 and 0.90 eV. The transition from C_6H_6 to C_6D_6 is accompanied by the expected reduction of ΔE_T. The low-temperature boundary values of ΔE_T amount to 0.13 and 0.67 eV; the T = 750 K boundaries are 0.32 and 0.85 eV. Tables 2 and 3 contain a second energetic parameter which visualizes the strong coupling between nuclear fluctuations and electronic transition energies, i.e., the standard deviation σ_i within a given set of $E_T(\mathbf{R})$ numbers. The calculated σ_i are between 0.17 eV (C_6D_6 at $T = 50$ K) and 0.31 eV (C_6H_6 at $T = 750$ K). The QMC simulations indicate clearly that the influence of the nuclear degrees of freedom is prevailingly of quantum mechanical origin. Classical thermal degrees of freedom are only of minor importance. This becomes clear when correlating ${}^{PI}\bar{E}_T$ at 50 K (i.e., bare quantum regime) with the CBO set E_T, as well as the high-temperature collection of the ${}^{PI}\bar{E}_T$ with the E_T numbers.

The isotope shift for the $^1B_{2u}$ transition in C_6H_6 and C_6D_6 has been measured by Robey and Schlag;[69] see also ref 70. The experimental shift of 203 cm^{-1} has been reproduced quantitatively by the present PIMC−ab initio approach which yields 202 cm^{-1}. Thus, it can be assumed that the isotope dependence of electronic transition energies in benzene isomers is adequately described by our QMC method. Also in the case of ethylene isomers it had been possible by PIMC simulations to reproduce experimental isotope shifts.[46] Christiansen et al.[27] have calculated an isotope shift of 186 cm^{-1} for the $^1B_{2u}$ transition in the $C_6H_6-C_6D_6$ pair. The method used in ref 27 belongs to the family of coupled cluster expansions. A convenient representation of the isotope shifts in the pair $C_6H_6-C_6D_6$ is given in Figure 5. Here, we have correlated the ${}^{PI}\bar{E}_T$ and ${}^{PI}\bar{f}_{osc}$ numbers

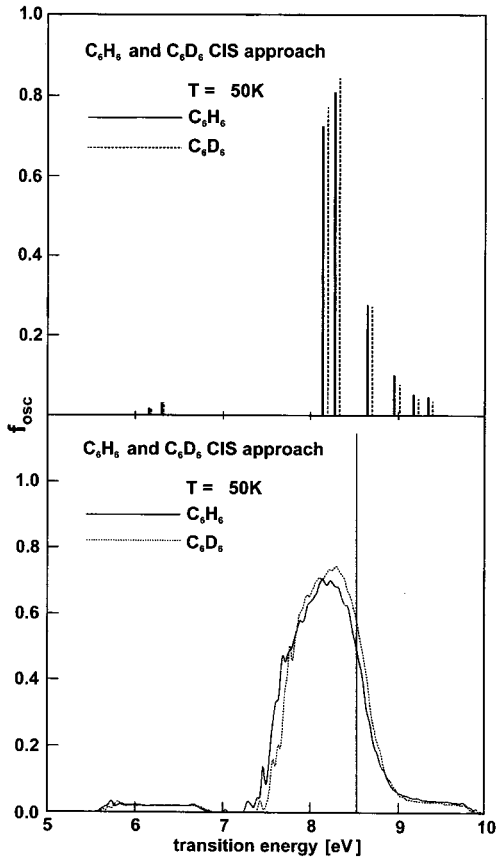

Figure 5. Comparison of the eight lowest singlet transition energies $^{PI}\bar{E}_T$ and intensities $^{PI}\bar{f}_{osc}$ (top diagram) as well as the associated distribution functions (bottom diagram) of C_6H_6 and C_6D_6 at $T = 50$ K. The C_6H_6 results have been given by full symbols, the C_6D_6 ones by broken symbols. The meaning of the full vertical line in the bottom diagram has been explained in the legend to Figure 3.

as well as the absorption profiles for the singlet transitions of the two benzene isomers. To sum up; despite the fact that the lowest singlet transitions arise from the $\pi \rightarrow \pi^*$ manifold, we find nonnegligible isotope effects when H is replaced by D. This indicates the nonvalidity of the $\pi-\sigma$ separability in planar π rings under the conditions of thermal equilibrium. The overall trends in Figure 5 are in line with the experimental $^1B_{2u}$ data of Robey and Schlag.[69]

With the help of the geometrical parameters in section IV it is straightforward to explain the reduction of the $^{PI}\bar{E}_T$ (FC maxima) relative to the E_T. We have emphasized that the anharmonicities in the nuclear potential $V(\mathbf{R})$ lead to bond lengths r_g in thermal equlibrium which exceed the r_e at the minimum of the PES. But such a spatial extension of a molecule with covalent bonding implies a destabilization of the bonding MOs and a stabilization of the antibonding virtual MOs. The energy differences between the occupied and unoccupied MOs, however, are key quantities of any CI approach. As a matter of fact, we find that the reduced one-particle gap in thermal equilibrium leads to ensemble averaged transition energies which are smaller than the E_T numbers (prerequisite: $\mathbf{R}_0$ geometry). Remember that the influence of the anharmonicities in $V(\mathbf{R})$ is enhanced with increasing temperature and decreasing isotope masses. This increase of the molecular volume in thermal equilibrium is also important when analyzing NMR parameters of hydrocarbon π systems. Relative to the magnetic shieldings at the $\mathbf{R}_0$ structure, we find a deshielding of the nuclei in thermal equilibrium. This topic has been studied in our recent PIMC−ab initio simulations of NMR parameters.[44,47]

Let us come to a rather provocative question. How is it possible to have a one-to-one correspondence between measured FC maxima of electronic transitions and single configuration results derived at the minimum of the ground state PES despite the neglect of the coupling between electrons and nuclei? On the basis of the present QMC results, only one answer seems to be possible, i.e., by error compensation (prerequisite: molecules with large nuclear delocalization and strong anharmonicities). Thus, it should be clear that improvements in H_{el} are not necessarily accompanied by results which are closer to experiment than results observed with a simpler design of H_{el}. Remember such a discussion in connection with the excited-state properties of C_2H_4.[46] At the end of the comparison between transition energies of the E_T and $^{PI}\bar{E}_T$ type, let us review some CI results derived for the $\mathbf{R}_0$ structure of C_6H_6.[23,30] Kitao and Nakatsuji have derived transition energies to the $^1B_{2u}$, $^1B_{1u}$, and $^1E_{1u}$ configurations which exceed the experimental FC maxima by 0.35, 0.40, and 0.52 eV.[23] Finley and Witek have observed an average error of 0.32 eV for the lowest intervalence transitions.[30] The combination of these single-configuration data with the present shift parameters ΔE_T (0.16, 0.22 and 0.31 eV for the $^1B_{2u}$, $^1B_{1u}$, and $^1E_{1u}$ configurations) yields singlet transition energies in benzene close to experiment. The consideration of the present ΔE_T parameters leads to differences between theory and experiment which are smaller than 0.2 eV. Remember that the vibrational corrections ΔE_T cause a reduction of the calculated FC maxima. We have adopted post HF calculations from the literature for our comparison in order to relate numerical results which belong to the same family of theoretical tools.

Now, let us analyze the oscillator strengths for the singlet transitions in C_6H_6 and C_6D_6 at the D_{6h} minimum (f_{osc}) and in thermal equilibrium ($^{PI}\bar{f}_{osc}$). The ensemble averages $^{PI}\bar{f}_{osc}$ are both a function of the temperature and of the isotope masses. At the beginning of this section, it has been mentioned that all singlet transitions are dipole-allowed if the nuclear fluctuations are taken into account in the CIS calculations. Tables 2 and 3 show that all $^{PI}\bar{f}_{osc}$ are $\neq 0$. The Kuhn−Thomas sum rule[71,72] implies a strong redistribution in the intensities of all singlet transitions in the step from a CBO calculation to an ABO simulation. Remember that only the transition to the $^1E_{1u}$ state of benzene is dipole-allowed in the point group D_{6h}. It is this transition which loses intensity under the influence of the nuclear fluctuations. The "intensity loss" in C_6H_6 caused by bare quantum fluctuations ($T = 50$ K) amounts to 33%. At $T = 750$ K, the loss in intensity amounts to 43%.

The $^{PI}\bar{f}_{osc}$ histograms in Figures 3 and 4 indicate some kind of "resonance" in the intensity transfer. The intensity transferred from the $^1E_{1u}$ transition (D_{6h} conditions) to a singlet transition dipole-forbidden under the same symmetry constraints, is reduced with increasing energetic separation between the $^1E_{1u}$ "intensity donor" and the "intensity acceptor". On the basis of the above discussion, it has been expected a priori that the transfer of "intensity" is enhanced with increasing temperature and reduced isotope mass. The $^{PI}\bar{f}_{osc}$ numbers in Tables 2 and 3 indicate that the standard deviation σ_i within the $f_{osc}(\mathbf{R})$ ensembles is of the same order of magnitude as the calculated intensities $^{PI}\bar{f}_{osc}$. An exception is the $^{PI}\bar{f}_{osc}$, σ_i pair for the dipole-allowed $^1E_{1u}$ transition.

Now let us reconsider the so-called "hot bands" in the optical spectrum of benzene, i.e., the dipole-forbidden $^1B_{2u}$ and $^1B_{1u}$ transitions.[4] In Figure 6, we have displayed the T-dependence of the distribution functions for the two lowest singlet transitions

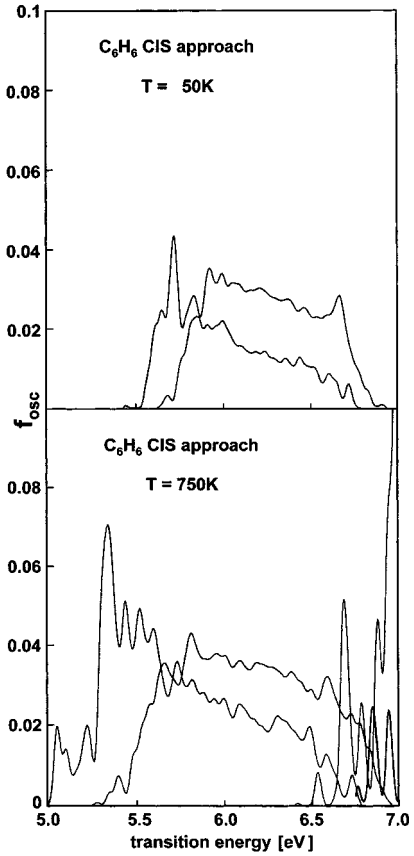

Figure 6. Distribution function for the two lowest singlet transitions of C_6H_6 as derived via PIMC ab initio CIS simulations. In the point group D_{6h} these transitions refer to the excited singlet states of $^1B_{2u}$ and $^1B_{1u}$ symmetry. They are dipole-forbidden for the point symmetry at the PES minimum. The top profiles have been derived for $T = 50$ K, the bottom ones for $T = 750$ K.

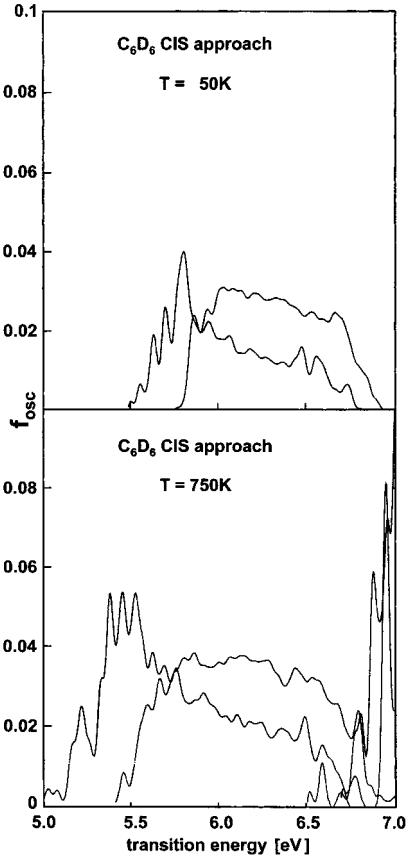

Figure 7. Distribution function for the two lowest singlet transitions of C_6D_6 at $T = 50$ and 750 K. See legend to Figure 6.

in C_6H_6. The C_6D_6 profiles have been portrayed in Figure 7. With the chosen f_{osc} scale, it is easy to identify the strong T-dependence of these "symmetry-forbidden" transitions. Their intensity is enhanced with increasing nuclear fluctuations.

The discussion of the oscillator strengths of electronic transitions in two theoretical degrees of sophistication, i.e., CBO versus ABO description, may lead to the suggestion that CBO calculations are not free of conceptual problems if a comparison with experiment is intended. In the single configuration picture, the geometry with the highest point symmetry compatible with the molecular topology is chosen as reference. With increasing anharmonicities in the nuclear potential $V(\mathbf{R})$ and increasing nuclear fluctuations (i.e., increasing deviations from the $\mathbf{R}_0$ structure) this choice becomes more and more questionable. The intensity redistributions under the influence of the nuclear degrees of freedom seem to be a severe obstacle for a comparison between calculated f_{osc} numbers and experiment.

At the end of this discussion section, let us compare ABO results $^{PI}\bar{E}_T$, $^{PI}\bar{f}_{osc}$ with the second set of single-point parameters E_T* and f_{osc}*. The latter single configuration numbers have been derived for thermally averaged bond lengths r_g of C_6H_6. $T = 50$ K results have been summarized in Table 4. In the derivation of the E_T* and f_{osc}* spectrum we have conserved the D_{6h} point symmetry of benzene. To sum up, the single point geometries have been defined by the combination of r_g coordinates with bondangles of the α_e type. Only the stretching of the benzene bonds in thermal equilibrium has been taken into account in the definition of the new "reference geometries". It is self-explanatory that the E_T* are somewhat smaller than the E_T.

TABLE 4: Electronic Excitation Energies E_T, $^{PI}\bar{E}_T$, and E_T* of C_6H_6 for the Eight Lowest Singlet States According to CIS Calculations in a 6-31G Basis Set[a]

state	minimum PES E_T	PIMC 50 K $^{PI}\bar{E}_T$	r_g 50 K E_T*	PIMC 750 K^{PI} $\bar{E}_T$	r_g 750 K E_T*
$^1B_{2u}$	6.32	6.16	6.25	5.98	6.21
$^1B_{1u}$	6.53	6.31	6.46	6.16	6.41
$^1E_{1u}$	8.53	8.14 8.28	8.44	7.88 8.06	8.39
$^1A_{2u}$	9.37	8.65	9.28	8.47	9.24
$^1E_{1g}$	9.50	8.95 9.17	9.32	8.80 9.03	9.29
$^1A_{1u}$	9.65	9.34	9.55	9.24	9.52

[a] The meaning of the energy parameters has been explained in the text. Remember that both E_T and E_T* are of the single nuclear configuration type. The E_T numbers refer to a D_{6h} structure with bondlengths of the r_e type. The E_T* numbers have been derived for bondlengths r_g ($T = 50$ and 750 K). The D_{6h} structure of C_6H_6 has been conserved in this approach. All transition energies in eV. The irreducible representations on the lhs correspond to the planar D_{6h} structure of C_6H_6.

Nevertheless, we have to recognize that the calculated "single configuration" shifts $\Delta E_T^* = E_T - E_T^*$ are small in comparison to the ensemble shifts ΔE_T which have been defined with the help of thermal mean values $^{PI}\bar{E}_T$. The conservation of the D_{6h} structure of C_6H_6 has been an obstacle for any redistribution in the oscillator strengths. In other words, the strong wave packet character of the nuclear wave function in molecules with light atoms prevents that CBO approaches can simulate excited-state properties under the conditions of thermal equilibrium. The differences between the E_T, f_{osc} and the E_T*, f_{osc}* sets are small in comparison to the differences between CBO and ABO results.

VI. Conclusions

In the present work, we have studied the excited singlet states of the two benzene isomers C_6H_6 and C_6D_6 under explicit consideration of the quantum and thermal degrees of freedom of the nuclei. To derive the finite-temperature properties of the excited singlet states of the two π molecules we have combined the Feynman path integral quantum Monte Carlo formalism with a configuration interaction scheme. With the PIMC method used vibrational corrections beyond the simple harmonic approximation become feasible. The largest number of vibrational correction schemes described in the literature is based on the harmonic approximationas well as on semiclassical simulation techniques. The theoretical setup used renders possible an adiabatic Born−Oppenheimer description of the molecular electronic excited states. In the derivation of the transition energies ${}^{PI}\bar{E}_T$, $E_T(\mathbf{R})$ and oscillator strengths in this degree of sophistication an ensemble averaging over 6000 different nuclear configurations has been performed. The singlet transitions for each molecular geometry, which have been chosen from the total QMC ensemble, are of the vertical Franck−Condon type. See again Figure 1 for a schematic representation of the general principles of the present approach.

The comparison of ensemble averaged results with single nuclear configuration data derived with the same electronic Hamiltoninan has led to insight into the intrinsic conceptual shortcomings of the widely employed CBO approximation. Here, the wave packet character of the nuclear wave function is neglected. The majority of CBO studies suffers additionally from a second unphysical approximation, i.e., the adoption of vibrationless $\mathbf{R}_0$ coordinates. In the present work as well as in some of our previous QMC studies, we have emphasized that the nuclear fluctuations on BO surfaces with strong anharmonicities lead to thermally averaged bond lengths r_g which are significantly larger than the hypothetical r_e lengths.[45−47] These differences explain that excited-state calculations for $\mathbf{R}_0$ coordinates with an optimum electronic HF Hamiltonian must yield transition energies larger than the experimental numbers. For C_6H_6 and C_6D_6, we have determined shift parameters ΔE_T which can exceed 0.7 eV.

Redistributions between the transition intensities ${}^{PI}\bar{f}_{osc}$ under the influence of the nuclear fluctuations are even more important than the observed shifts ΔE_T. For the rigid D_{6h} symmetry of benzene (CBO description), only the singlet transition to the ${}^1E_{1u}$ state is dipole-allowed in the 6-31G basis used. Such a strong symmetry constraint is no longer operative in thermal equilibrium. The nuclear fluctuations lead to molecular geometries with point symmetries much lower than D_{6h}; see the pdf plots in Figure 2. It is this symmetry reduction of the benzene configurations under the influence of the nuclear degrees of freedom which renders possible redistributions in the intensity of the singlet transitions. According to the Kuhn−Thomas sum rule the total intensity for all electronic transitions must be roughly the same in the static CBO approximation with its D_{6h} constraint and in the dynamical ABO picture. This conservation rule however implies that transitions which are dipole-allowed for the point symmetry at the minimum of the BO surface must lose intensity under the conditions of thermal equilibrium; vice versa for transitions which are dipole-forbidden for the D_{6h} case. We have shown that the nuclear degrees of freedom are prevailingly of quantum mechanical character; classical thermal fluctuations are of only minor importance. An exception is the sizable *T*-dependence of the intensities of the first two singlet transitions. In the point group D_{6h} these transitions are of ${}^1B_{2u}$ and ${}^1B_{1u}$ symmetry. The isotope shift for the ${}^1B_{2u}$ transition in the $C_6H_6-C_6D_6$ pair has been considered in detail in the present work. A quantitative reproduction of the experimental result has been possible.

It has been a central topic of the present work to emphasize the strong wave packet character of the nuclear wave function in molecules with light atoms and strong anharmonicities in the nuclear potential. Both factors restrict the computational capabilities of any single nuclear configuration approach. The technical limitations of the present QMC simulations have been mentioned several times. From a physical point of view it, seems to be desirable to consider non-FC transitions and to study mode-selective couplings. The evaluation of such parameters would require modifications in the PIMC step of our theoretical approach. The atomic displacements allowed in mode-selective simulations must belong to the normal modes of the molecule studied. Non-FC effects would require the evaluation of a separate BO surface for each electronic state analyzed. From the technical point of view, the following seems to be desirable: Self-consistency between PIMC and ab initio CIS step, extension of the atomic basis, many-body approaches beyond the CIS method. Despite all technical constraints we are convinced that the present study has offered physical insight into the excited-state properties of benzene isomers.

Acknowledgment. The present work has been supported by CICYT (Spain) under Contract No. BFM-2000-1318 (R.R.). We are grateful to Dr. S. Philipp for critically reading the manuscript.

References and Notes

(1) Hehre, W. J.; Radom, L.; Schleyer, P.v.R. *Ab Initio Molecular Orbital Theory*; Wiley: New York, 1986.
(2) *Reviews in Computational Chemistry*; Lipkowitz, K. B., Boyd, D. B., Eds.; VCH: Weinheim, 1990, 1991; Vols. 1, 2.
(3) Foresman, J. B.; Fritsch, M. J. *Exploring Chemistry with Electronic Structure Methods*; Gaussian: Pittsburgh, PA, 1996.
(4) Herzberg, G. *Electronic Spectra of Polyatomic Molecules*; van Nostrand: New York, 1966.
(5) Heller, E. J. *J. Chem. Phys.* **1978**, *68*, 3891.
(6) Heller, E. J. *Acc. Chem. Res.* **1981**, *14*, 368.
(7) Reimers, J. R.; Wilson, K. R.; Heller, E. J. *J. Chem. Phys.* **1983**, *79*, 4750.
(8) Weide, K.; Schinke, R. *J. Chem. Phys.* **1987**, *87*, 4627.
(9) Weide, K.; Schinke, R. *J. Chem. Phys.* **1989**, *90*, 7150.
(10) Schinke, R. *Collission Theory for Atoms and Molecules*; Gianturco, F., Ed.; Plenum: New York, 1**989**.
(11) Mebel, A. M.; Chen, Y.-T.; Lin, S.-H. *Chem. Phys. Lett.* **1996**, *258*, 53.
(12) Mebel, A. M.; Chen, Y.-T.; Lin, S.-H. *J. Chem. Phys.* **1996**, *105*, 9007.
(13) Mebel, A. M.; Hayashi, M.; Lin, S.-H. *Chem. Phys. Lett.* **1997**, *274*, 181.
(14) Hayashi, M.; Mebel, A. M.; Liang, K. K.; Lin, S. H. *J. Chem. Phys.* **1998**, *108*, 2044.
(15) Davidson, E. R.; Jarzecki, A. A. *Chem. Phys. Lett.* **1998**, *285*, 155.
(16) Cardenas, A. E.; Krems, R.; Coalson, R. D. *J. Phys. Chem. A* **1999**, *103*, 9469.
(17) Ben-Nun, M.; Martínez, T. J. *J. Phys. Chem. A* **1999**, *103*, 10 517.
(18) Toniolo, A.; Persico, M.; Pitea, D. *J. Phys. Chem. A* **2000**, *104*, 7278.
(19) Fischer, G. *Vibronic Processes in Inorganic Chemistry*; Flint, C. D., Ed.; Kluwer: Dordrecht, 1989.
(20) Franck, J. *Trans. Faraday Soc.* **1925**, *21*, 536.
(21) Condon, E. U. *Phys. Rev.* **1928**, *32*, 858.
(22) Foresman, J. B.; Schlegel, H. B. *Molecular Spectroscopy: Recent Experimental and Computational Advances, NATO-ASI Series*; Fausto, R., Ed.; Kluwer: Dordrecht, 1993.
(23) Kitao, O.; Nakatsuji, H. *J. Chem. Phys.* **1987**, *87*, 1169.
(24) Palmer, M. H.; Walker, I. *Chem. Phys.* **1989**, *133*, 113.
(25) Roos, B. O.; Andersson, K.; Fülscher, M. P. *Chem. Phys. Lett.* **1992**, *192*, 5.
(26) Del Bene, J.; Watts, J. D.; Bartlett, R. J. *J. Chem. Phys.* **1997**, *106*, 6051.

(27) Christiansen, O.; Stanton, J. F.; Gauss, J. *J. Chem. Phys*. **1998**, *108*, 3987.
(28) Stratmann, E.; Scuseria, G. E.; Frisch, M. J. *J. Chem. Phys*. **1998**, *109*, 8218.
(29) Adamo, C.; Scuseria, G: E.; Barone, V. *J. Chem. Phys*. **1999**, *111*, 2889.
(30) Finley, J. P.; Witek, H. A. *J. Chem. Phys*. **2000**, *112*, 3958.
(31) Heinze, H. H.; Görling, A.; Rösch, N. *J. Chem. Phys*. **2000**, *113*, 2088.
(32) Pickett, L. W.; Muntz, M.; McPherson, E. M. *J. Am. Chem. Soc.* **1951**, *73*, 4872.
(33) Doering, J. P. *J. Chem. Phys*. **1969**, *51*, 2866.
(34) Koch, E. E.; Otto, A. *Chem. Phys. Lett.* **1972**, *12*, 476.
(35) Pantos, E.; Philis, J.; Bolovinos, A. J. *Mol. Spectrosc.* **1978**, *72*, 36.
(36) Feynman, R. P.; Hibbs, A. R. *Quantum Mechanics and Path Integrals*; McGraw-Hill: New York, 1965.
(37) Feynman, R. P. *Statistical Mechanics*; Benjamin: New York, 1972.
(38) Kleinert, H. *Pfadintegrale*; Wissenschaftsverlag: Mannheim, **1993**.
(39) Berne, B. J.; Thirumalai, D. *Annu. Rev. Phys. Chem.* **1987**, *37*, 401.
(40) Gillan, M. J. *Computer Modelling of Fluids, Polymers and Solids*; Catlow, C. R. A., Parker, S. C., Allen, M. P., Eds.; Kluwer: Dordrecht, 1990, p 155.
(41) Ramírez, R.; Schulte, J.; Böhm, M. C. *Chem. Phys. Lett.* **1997**, *275*, 377.
(42) Böhm, M. C.; Ramírez, R.; Schulte, J. *Chem. Phys*. **1998**, *227*, 271.
(43) Ramírez, R.; Hernández, E.; Schulte, J.; Böhm, M. C. *Chem. Phys. Lett.* **1998**, *291*, 44.
(44) Böhm, M. C.; Schulte, J.; Ramírez, R. *Chem. Phys. Lett.* **2000**, *332*, 117.
(45) Böhm, M. C.; Schulte, J.; Hernández, E.; Ramírez, R. *Chem. Phys.* **2001**, *264*, 371.
(46) Ramírez, R.; Schulte, J.; Böhm, M. C. *Mol. Phys.* **2001**, *99*, 1249.
(47) Böhm, M. C.; Schulte, J.; Ramírez, R. *Int. J. Quantum Chem.* **2002**, *86*, 280.
(48) Barnett, R. N.; Landman, U. *Phys. Rev. B* **1993**, *48*, 2081.
(49) Marx, D.; Parrinello, M. *Z. Phys. B* **1994**, *95*, 143.
(50) Cheng, H.-P.; Barnett, R. N.; Landman, U. *Chem. Phys. Lett*. **1995**, *237*, 161.
(51) Valladares, R. M.; Fisher, A. J.; Hayes, W. *Chem. Phys. Lett.* **1995**, *242*, 1.
(52) Marx, D.; Tuckerman, M. E.; Hutter, J.; Parrinello, M. *Nature* **1999**, *397*, 661.
(53) Gaussian 94, Revision D.4, Fritsch, M. J.; Trucks, G. W.; Schlegel, H. B.; Gill, P. M. W.; Johnson, B. G.; Robb, M. A.; Cheeseman, J. R.; Keith, T.; Petersson, G. A.; Montgomery, J. A.; Raghavachari, K.; Al-Laham, M. A.; Zakrzewski, V. G.; Ortiz, J. V.; Foresman, B. J.; Cioslowski, J.; Stefanov, B. B.; Nanayakkara, A.; Challacombe, M.; Peng, C. Y.; Ayala, P. A.; Chen, W.; Wong, M. W.; Andres, J. L.; Replogle, E. S.; Gamperts, R.; Martin, R. L.; Fox, D. J.; Binkley, J. S.; Defrees; D. J.; Baker, J.; Stewart, J. P.; Head-Gordon, M.; Gonzales, C.; Pople, J. A. Gaussian: Pittsburgh, PA, 1995.
(54) Karasawa, N.; Dasgupta, S.; Goddard, III, W. A. *J. Phys. Chem.* **1991**, *95*, 2260.
(55) Schulte, J.; Ramírez, R.; Böhm, M. C. *Chem. Phys. Lett.* **2000**, *322*, 257.
(56) Ramírez, R.; Böhm, M. C. *J. Phys.*: *Condens. Mater*. **1995**, *7*, 4847.
(57) Böhm, M. C.; Ramírez, R. *J. Phys. Chem*. **1995**, *99*, 12401.
(58) Rowe, W. F.; Doverst, R. W.; Wilson, E. B. *J. Am. Chem. Soc.* **1976**, *98*, 8, 4021.
(59) Seliskar, C. J.; Hoffmann, R. E. *J. Mol. Spectrosc.* **1981**, *88*, 30.
(60) Cao, J.; Berne, B. J. *J. Chem. Phys*. **1993**, *99*, 2902.
(61) Metropolis, N.; Rosenbluth, A. W.; Rosenbluth, M. N.; Teller, A. H.; Teller, E. *J. Chem. Phys*. **1953**, *21*, 20.
(62) Ramírez, R.; Böhm, M. C.; Schulte, J. *J. Phys. B*, submitted for publication.
(63) Pollock, E. L.; Ceperly, D. M. *Phys. Rev. B* **1984**, *30*, 2555.
(64) Coalson, R. D.; Freeman, D. L.; Doll, J. D. *J. Chem. Phys*. **1985**, *85*, 4567.
(65) Graybeal, J. D. *Molecular Spectroscopy*; McGraw-Hill: New York, 1988.
(66) Astrand, P.-O.; Ruud, K.; Mikkelsen, V.; Helgaker, T. *J. Chem. Phys*. **1999**, *110*, 9463.
(67) Astrand, P.-O.; Ruud, K.; Taylor, P. R. *J. Chem. Phys*. **2000**, *112*, 2655.
(68) Kuchitsu, K. *Accurate Molecular Spectroscopy*; Domenicano, A., Hargittai, I., Eds.; Oxford University Press: Oxford, 1992, p 14.
(69) Robey, M. J.; Schlag, E. W. *J. Chem. Phys*. **1977**, *76*, 2775.
(70) Sur, A.; Knee, J.; Johnson, P. *J. Chem. Phys*. **1982**, *77*, 654.
(71) Davidov, A. S. *Quantum Mechanics*; Pergamon Press: Oxford, 1976.
(72) Atkins, P. W. *Molecular Quantum Mechanics*; Oxford University Press: Oxford, 1983.